

OPTICAL CHARACTERIZATION OF TiO₂-Ge NANOCOMPOSITE FILMS OBTAINED BY REACTIVE MAGNETRON SPUTTERING

A. SLAV*

*National Institute of Materials Physics, 105 bis Atomistilor Street, Magurele
077125, Romania*

The optical band gaps of the nanocomposite TiO₂-Ge thin films deposited by reactive co-sputtering method onto quartz and silicon substrates at different oxygen partial pressures have been investigated by the optical characterization method. Using 2%, 4% and 6% oxygen dilution in argon, an atomic content of 3%, 22% and 35% germanium in the TiO₂ oxide matrix was obtained. Structural characterization of layers was performed by X-ray diffraction and the result revealed that no crystallization phenomena have occurred after the annealing at 700 °C. When increasing the annealing temperature, at 750 °C the TiO₂ anatase phase crystallizes and subsequently it partially convert to the rutile polymorph (at 800 °C). The optical band gaps were analyzed using Tauc plot formula for direct and indirect transitions gap. Intermediate energy levels appear in the TiO₂ energy gap and a slight increasing of the indirect transitions gap with germanium content was noticed.

(Received May 4, 2011; Accepted May 11, 2011)

Keywords: TiO₂-Ge nanocomposite, magnetron sputtering, optical band gap, XRD, FT-IR

1. Introduction

Considerable research of titanium dioxide (TiO₂), largely employed in chemistry, comes from its multifunctional properties making it one of the most investigated metal oxides. This is a cheap semiconductor with striking photocatalytic capabilities in several heterogeneous reactions. Applications in the field of electronic devices, decomposition of polluting compound, protection of artwork from oxidation, medical bioengineering, photoreactions for specific syntheses, solar energy conversion with optimal quantum yields, and production of molecular hydrogen from water were generating along the years a substantial scientific literature [1]. The list of TiO₂ applications is still growing due to peculiar properties of this promising material emerging at the nanoscale [2,3].

TiO₂ is a material of increasing interest especially in electronics and optoelectronics, with applications in high-k dielectrics, solar cells, and photocatalysis [4–8]. Rutile TiO₂ has a wide band gap of 3.1 eV and shows a tendency for unintentional n-type conductivity [9–15].

Optical properties of TiO₂ include a wide band gap, high transparency in the visible spectrum and a high refractive index over a wide spectral range (from ultraviolet to the far infrared). Nanocrystalline titania (TiO₂) is also a promising semiconductor for applications based on its photoconductivity. The reported optical gap of TiO₂ is in the range of 3-3.6 eV [16-19] corresponding to the ultraviolet region of the solar spectrum. The titania-germanium (TiO₂-Ge) nanocomposites, defined as a TiO₂ matrix which include a rather uniform distribution of Ge nanodots, has recently risen as an alternative solution in the solar cells [20]. Applications TiO₂-Ge nanostructures have a great advantage because their synthesis is relatively cheap and they offer the promise of high efficiency for solar photon conversion. For their synthesis, the reactive magnetron sputtering technique is commonly used. Today the TiO₂ is widely used as dye sensitized, but the TiO₂-Ge nanocomposite could also represent a good alternative [21]. However, the charge

* Corresponding author: slav@infim.ro

transport and instability of the organic complex in the dye, still represent major problems.

2. Experimental

The experiments were carried out using a magnetron sputtering system equipped with balanced magnetron cathodes (110 mm diameter, 55 mm plasma ring) operating in radio-frequency at 1.78 MHz. Silicon wafers (100) and fused silica were used as substrates. Prior the deposition, substrates were cleaned by ex situ chemical procedures and in situ argon plasma etching. A titanium disc with germanium square pieces fixed on its sputtering racetrack ring was used as a cathode target (Ti:Ge area ratio=15).

Table 1 The EDX chemical composition for the as-deposited TiO₂-Ge samples vs. deposition conditions.

Reactive gas conc.	Ti (at. %)	Ge (at. %)
2%	97	3
4%	78	22
6%	65	35

The deposition was performed at a constant working pressure of 0.3 Pa and substrate temperature of maximum 150°C. Argon was introduced in the deposition chamber as a working gas and oxygen diluted in argon (2–10%) was used as a reactive gas. The total gas flow during deposition was 45 sccm [22, 23]. The TiO₂-Ge nanocomposite films were obtained by co-sputtering. The sputtering rate, Ge/Ti molar ratio, along with their structural and optical features were tailored by varying the oxygen dilution in argon (Table 1). Magnetron sputtering deposited films are usually amorphous. In order to induce their crystallization, a post-deposition thermal annealing was performed in air at 650, 700, 750 and 800°C, respectively. The as-prepared thin films were characterized by X-ray diffraction (XRD), energy-dispersive X-ray spectroscopy (EDX), Fourier transform infrared (FT-IR) spectroscopy and UV-visible spectroscopy (UV-Vis).

3. Results and discussion

As mentioned above, TiO₂-Ge films were prepared from a Ti-Ge target by reactive co-sputtering using three different oxygen dilutions. One can expect that the structural properties of the films would be influenced by the sputtering conditions and the thermal annealing[24].

In Table.1 it is shown the elemental composition of TiO₂-Ge nanocomposite sputtered thin films, estimated by EDX spectroscopy. One can notice a linear dependence between the oxygen dilution in the working atmosphere and Ge concentration into the TiO₂ matrix. The results suggest that the ratio of Ge into TiO₂ matrix can be adjusted by controlling the working atmosphere, the oxidizing rate of Ti and thus its sputtering yield. This process is explained by the preferential oxidation of Ti, thus leaving Ge in the elemental form, due to the difference of electronegativity between Ti (1.54 Pauling) and Ge (2.01 Pauling) [25].

The XRD patterns of the films are plotted comparatively in Fig. 1 where the peaks were identified using the ICDD database (TiO₂-anatase – ICDD: 70-6826, TiO₂-rutile – ICDD: 82-514 and GeO₂ – ICDD: 85-1519). One can notice that the annealing temperature changes significantly the microstructure of the composite films. The XRD patterns show that no crystallization phenomena have occurred after the annealing at 700°C. When increasing the annealing temperature to 750°C, TiO₂-anatase phase crystallized. It is well-known that the anatase phase is thermodynamically less stable than the rutile phase, and thus by increasing the annealing temperature to 800°C it partially converts to the rutile polymorph (Fig.1). It was noticed that the experimental diffraction peaks of both anatase and rutile are shifted towards higher angles relative to the reference ICDD positions, accompanied by the changes of relative intensities. These modifications of the diffraction patterns of titanium oxides suggest the dilution of Ge atoms in the anatase and rutile lattice, respectively. This shift is slightly noticeable in the samples with 3% Ge and 22% Ge annealed at 750°C and 800°C respectively.

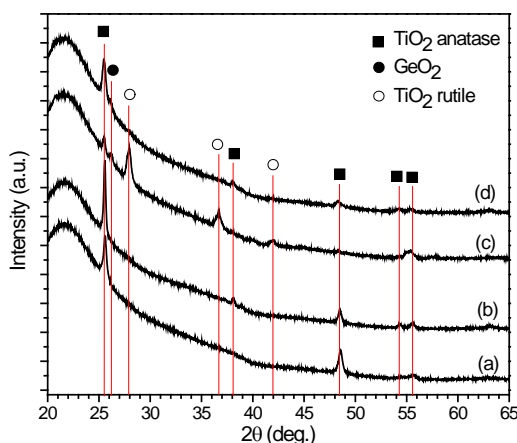


Fig. 1 XRD patterns of TiO_2 -Ge nanocomposite films deposited by magnetron sputtering at various oxygen dilution as reactive gas: 2% O_2 , annealed at 750 °C-(b) and 800 °C-(c) and 4% O_2 annealed at 750 °C-(a) and 800 °C-(d)

The crystallite size of Ge and TiO_2 was evaluated using Scherrer's formula $D = \frac{\lambda}{\beta \cos \theta}$,

where D is the mean crystallite size in Å, λ is the wavelength of Cu $K\alpha$ X-rays (1.5418 Å), β is the size broadening of diffraction line (integral breadth) in radians and θ is the diffraction angle. Value of β is determined from the experimental line width by subtracting the instrumental profile width. The instrumental profile was calibrated using a standard corundum sample (NIST SRM 1976). Neglecting the possible strain broadening of the peaks, the following average crystallite sizes were obtained: 36 nm for anatase in samples with 3% Ge (annealed at 750°C and 800°C), 25 nm for anatase in samples with 22% Ge (annealed at 750°C and 800°C), 19 nm for rutile in the sample with 3% Ge (annealed at 800°C) and around 35 nm for GeO_2 in the samples annealed at 800°C.

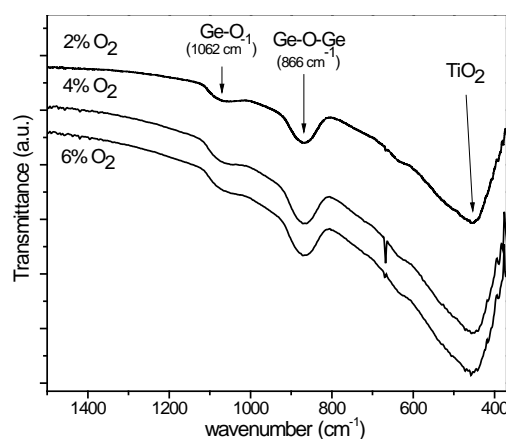


Fig. 2 FT-IR spectra of TiO_2 -Ge nanocomposite films obtained by reactive co-sputtering (2%, 4% and 6% O_2 dilutions) after annealing at 800 °C

The FT-IR spectra in transmission mode for the films deposited on Si(100) wafer for TiO_2 -Ge films with 3%, 22% and 35% atomic content of Ge are shown in Fig.2. The atomic content corresponds to different values of oxygen partial pressure as shown in Table 1. The spectra display features corresponding to complex vibrations due to TiO_2 and GeO_2 , with three strong broad bands positioned at 1062 cm^{-1} (attributed to Ge-O vibrations), 866 cm^{-1} (Ge-O-Ge vibrations), and 450 cm^{-1} (assigned to TiO_2 vibrations) [26]. One can also remark that overall spectra intensity is increasing with the annealing temperature, as well as the shift to higher wave numbers. These displacements could be due to the presence of Ge atoms into the TiO_2 lattice, that also indicates a certain degree of modification in the TiO_2 lattice, which could be correlated with the compositional and crystalline changes.

It is well-known from literature that apparent energy band gap of TiO₂-Ge composite thin films changes with the film thickness [27], deposition technique [29], and annealing temperature [30] due to the formation of nanoparticles [27], nanoporosity[31], and a oxide lattice [28,29] causing quantum confinement effects associated with nanostructures [27,28,29]. In order to obtain information about the energy band gap of TiO₂-Ge and also about the influence of deposition conditions the absorbance spectra of the thin films with different content of Ge were recorded. The optical absorption edge was analyzed with Tauc equation [32],

$$\alpha h\nu = A(h\nu - E_g)^m,$$

where A is the optical constant, α is the absorption coefficient, E_g is the optical band gap and m value is 1/2 for direct transitions and 2 for indirect transitions.

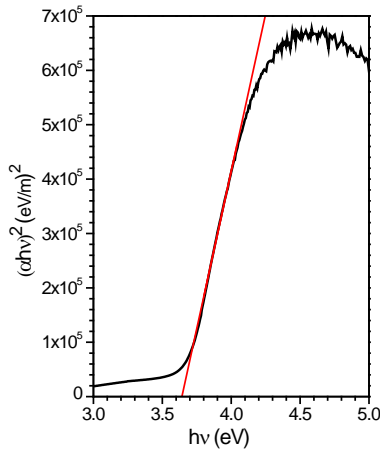


Fig. 3 Variation of $(\alpha h\nu)^2$ with excitation energy $h\nu$ for a TiO₂ film to identify direct transitions

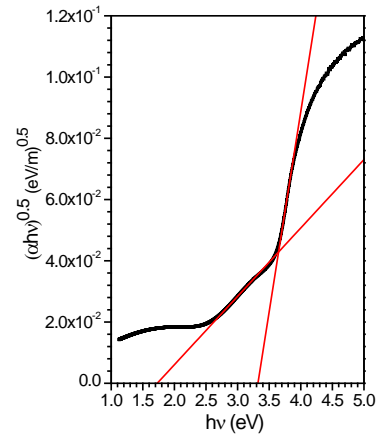


Fig. 4 Variation of $(\alpha h\nu)^{0.5}$ with excitation energy $h\nu$ for a TiO₂ film to identify indirect transitions

We analyze first the TiO₂ films annealed at 800°C, deposited in the same conditions as TiO₂-Ge. Variation of $(\alpha h\nu)^2$ with photon energy $h\nu$ for deposited films is shown in Fig.3. One can observe that the plots are linear over a wide range of photon energy, suggesting direct transitions. The direct band gap energy E_g of 3.6 eV, was calculated using Tauc Eq. for $m=1/2$, from the intersections of the straight line with the energy axis. To evaluate the indirect band gaps of TiO₂ we plotted the variation of $(\alpha h\nu)^{1/2}$ versus photon energy $h\nu$ (Fig.4). The fit with Tauc equation with $m=2$ gives 3.20 eV, corresponding to the indirect band gap. All band gap values obtained for TiO₂ thin films prepared by magnetron sputtering are in good agreement with the reported values from the scientific literature, 3.60–3.75 eV for the direct band gap and 3.05–3.20 eV for the indirect band gap respectively [33].

In Fig. 5 and Fig.6 we analyze the variation of $(\alpha h\nu)^2$ function on the photon energy $h\nu$ for the nanocomposite titania TiO₂-Ge with 3% respectively 22% content of Ge (atomic percent), annealed at 800°C. Using the same algorithm described above we evaluated the direct band gap from Tauc equation. For nanocomposite with 3% Ge in Fig. 5 the calculated direct band gap is 3.75 eV. For nanocomposite with 22% germanium in Fig.6 the direct band gap is 3.72 eV. One can notice only a slight modification of the direct band of 0.03eV when Ge atomic content is varied from 3% to 22%. This absorption edges of TiO₂-Ge match the optical edge of undoped TiO₂. This means that Ge atoms concentration is too small to influence the optical direct spectrum of the TiO₂ host matrix.

In the insets of Fig. 5 and Fig. 6 we plot the variation of $(\alpha h\nu)^2$ for smaller values of photon energy $h\nu$. We notice the nonlinear behavior, not seen in the undoped titania. It suggests the presence of the electron indirect transition.

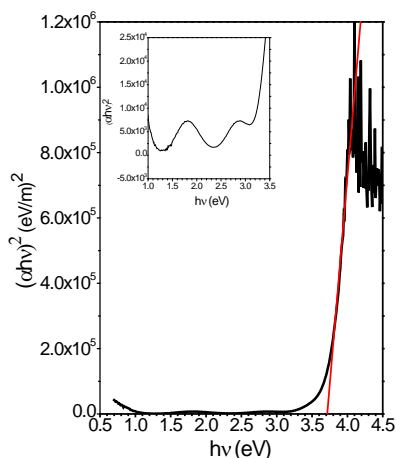


Fig. 5 Variation of $(\alpha h\nu)^2$ with excitation energy $h\nu$ for a TiO_2 -Ge film with 3% Ge (at. %) to identify direct transitions

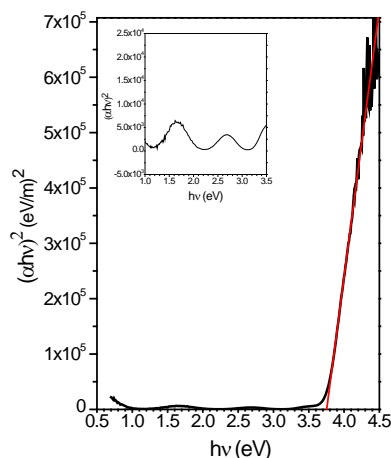


Fig. 6 Variation of $(\alpha h\nu)^2$ with excitation energy $h\nu$ for a TiO_2 -Ge film with 22% Ge (at. %) to identify direct transitions

The indirect band gap for nanocomposite titania doped with 3% and 22% (at. %) germanium was calculated from Fig.7 and Fig.8 respectively. From Fig.7 we obtained the indirect gap energy $E_g = 3.27$ eV for the most pronounced absorption (highest absorbance A) and other two indirect transitions with energy gap 1.91 eV and 1.06 eV. In Fig.8 with increasing germanium content we notice that the most pronounced indirect gap increased from 3.27 eV (3% at. cont.) to 3.45 eV (22% at. cont.). We noticed other three indirect transitions with the gap energy 2.95 eV, 1.96 eV and 0.9 eV respectively [35].

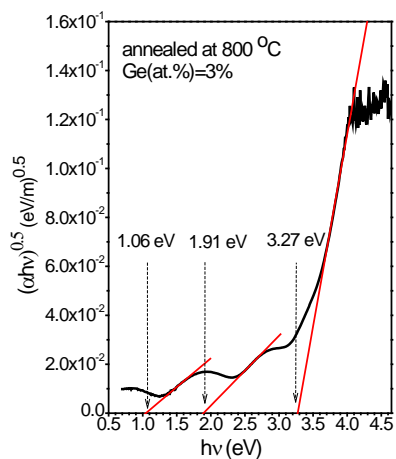


Fig. 7 Variation of $(\alpha h\nu)^{0.5}$ with excitation energy $h\nu$ for a TiO_2 -Ge film with 3% Ge (at. %) to identify direct transitions

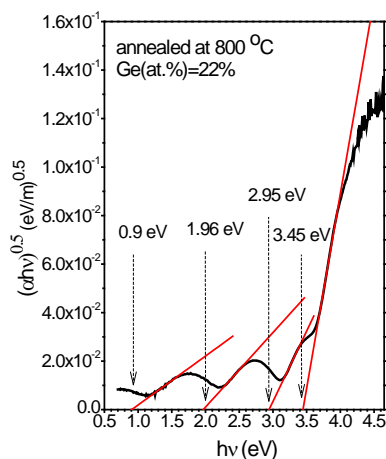


Fig.8 Variation of $(\alpha h\nu)^{0.5}$ with excitation energy $h\nu$ for a TiO_2 -Ge film with 22% Ge (at. %) to identify direct transitions

4. Conclusions

The nanocomposite titania doped with germanium was prepared by reactive magnetron sputtering using co-deposition method. Germanium content was modulated by the partial pressure of oxygen in working atmosphere. It was proved that the presence of Ge in TiO_2 matrix produces the shift of the diffraction peaks. The results obtained from optical absorption measurements analysed show that the amorphous TiO_2 matrix gives the major contribution to the direct band gap. The indirect gap slowly increases with Ge content. The indirect energy edges could also appear due to the contribution of different clusters/defects present in the amorphous matrix.

Acknowledgements

The work was supported by Romanian National Authority for Scientific Research through the Core Program Contract PN09-45. We also thank dr.I. Pasuk for the support with XRD measurements.

References

- [1] U. Diebold, Surf. Sci. Rep. **48**, 53 (2003).
- [2] O. Carp, C. L. Huisman, and A. Reller, Prog. Solid State Chem. **32**, 33 (2004).
- [3] M. Fernández-García, A. Martínez-Arias, J. C. Hanson, and J. A. Rodriguez, Chem. Rev. (Washington, D.C.) **104**, 4063 (2004).
- [4] G. Wilk, R. Wallace, and J. Anthony, J. Appl. Phys. **89**, 5243 (2001).
- [5] B. O'Regan and M. Grätzel, Nature (London) **353**, 737 (1991)
- [6] A. Fujishima and K. Honda, Nature (London) **238**, 37 (1972).
- [7] A. L. Linsebigler, G. Lu, and J. T. Yates, Jr., Chem. Rev. (Washington, D.C.) **95**, 735 (1995).
- [8] N. Umezawa, A. Janotti, P. Rinke, T. Chikyow, and C. G. Van de Walle, Appl. Phys. Lett. **92**, 041104 (2008).
- [9] E. Yagi, R. R. Hasiguti, and M. Aono, Phys. Rev. B **54**, 7945 (1996).
- [10] J. Yahia, Phys. Rev. **130**, 1711 (1963).
- [11] C. J. Kevane, Phys. Rev. **133**, A1431 (1964).
- [12] L. Forro, O. Chauvet, D. Emin, L. Zuppiroli, H. Berger, and F. Levy, J. Appl. Phys **75**, 633 (1994).
- [13] J. Nowotny, M. Radecka, M. Rekas, S. Sugihara, E. R. Vance, and W. Weppner, Ceram. Int. **24**, 571 (1998).
- [14] M. K. Nowotny, T. Bak, and J. Nowotny, J. Phys. Chem. B **110**, 16270 (2006).
- [15] P. Kofstad, J. Less-Common Met. **13**, 635 (1967).
- [16] D Reyes-Coronado, G Rodriguez-Gattorno, M E Espinosa-Pesqueira, C Cab, R de Coss and G Oskam, Nanotechnology **19**, 145605 (2008) (10pp)
- [17] Young Ran Park, Kwang Joo Kim, Thin Solid Films **484**, 34 (2005)
- [18] S. Sankar and K. G. Gopchandran, Cryst. Res. Technol. **44**(9), 989 (2009)
- [19] P. Madhu Kumar, S. Badrinarayanan, Murali Sastry, Thin Solid Films **358**, 122 (2000).
- [20] S. Chatterjee, Nanotechnology **19**, 265701 (2008) (9pp)
- [21] S. Chatterjee, Solar energy **82**, 95-99 (2008)
- [22] Cheol Ho Heo, Soon-Bo Lee, Jin-Hyo Boo, Thin Solid Films **475**, 183 (2005)
- [23] P. Baroch, J. Musil, J. Vlcek, K.H. Nam, J.G. Han, Surface & Coatings Technology **193**, 107 (2005).
- [24] P. Barquinha, L. Pereira, H. A'guas, E. Fortunato, R. Martins, Materials Science in Semiconductor Processing **7**, 243 (2004)
- [25] S. Chatterjee, J. Phys. D: Appl. Phys. **41**, 055301 (2008) (9pp)
- [26] G. Socrates, "Infrared and Raman characteristics group frequencies", Wiley (2001)
- [27] S. Tripathi, R. Brajpuriya, A. Sharma, A. Soni, G.S. Okram, S.M. Chaudhari, T. Shripathi, J. Nanosci. Nanotechnol. **8**(6), 2955 (2008)
- [28] E.B. Gorokhov, V.A. Volodin, D.V. Marin, D.A. Orekhov, A.G. Cherkov, A.K.Gutakovskii, V.A. Shvets, A.G. Borisov, M.D. Efremov, Semiconductors **39**, 1168 (2005)
- [29] A. Welte, C. Waldauf, C. Brabec, P.J. Wellmann, Thin Solid Films **516**, 7256 (2008)
- [30] A.F. Khan, M. Mehmood, A.M. Rana, T. Muhammad, Appl. Surf. Sci. (2009)
- [31] P.A. Calderon, M.C. Irisson, C.-W. Chen, Nanoscale Res. Lett. **3**, 55 (2008)
- [32] J.Tauc al., 627 Phys. Stat. Sol. **15**, 627 (1966)
- [33] S.Kowalczyk et al, Sol. St. Comm. **23**,161 (1977)
- [34] D.C.Cronemeyer, Phys. Rev. **87**, 876 (1952)
- [35] A. Faheem Khan, M. Mehmood, M. Aslam, S.I. Shah, Journal of Colloid and Interface Science **343**, 271 (2010).